Recent review on electron transport layers in perovskite solar cells

Shini Foo[1, 2, 3, 4], M. Thambidurai[1, 2], P. SenthilKumar[5], R. Yuvakkumar[6], Yizhong Huang*[4], and Cuong Dang*[1,23]*

1. Centre for OptoElectronics and Biophotonics (COEB), School of Electrical and Electronic Engineering, The Photonics Institute (TPI), Nanyang Technological University Singapore, 50 Nanyang Avenue, Singapore 639798, Singapore.
2. Energy Research Institute @NTU (ERI@N), Research Techno Plaza, X-Frontier Block, Level 5, 50 Nanyang Drive, 637553, Singapore.
3. Interdisciplinary Graduate School, Nanyang Technological University, Singapore 639798, Singapore
4. School of Materials Science and Engineering, Nanyang Technological University, 50 Nanyang Avenue, 639798, Singapore.
5. Department of Chemical Engineering, Sri Sivasubramaniya Nadar College of Engineering, Chennai, 603110, India
6. Department of Physics, Alagappa University, Karaikudi, 630 003, Tamil Nadu, India.

* Corresponding author details: senthilkumarp@ssn.edu.in (P. Senthil Kumar);

yzhuang@ntu.edu.sg (Yizhong Huang); hcdang@ntu.edu.sg (Cuong Dang)

Abstract

Organic-inorganic perovskite solar cells demonstrate immense potential for future photovoltaic application due to their remarkable efficiency advancements competitively low-cost. To unlock the full capability of perovskite, developments to the neighbouring layers play immense roles in the ultimate performance of a perovskite solar device. Here, a brief review comprising of the advancements and roles of electron transport layers (ETLs) is discussed. In addition, the effects of ETL on the charge transport, hysteresis, and stability of perovskite solar devices, along with high−performing examples, are also explored.

Keywords: solar energy materials; semiconductors; election transport layer; hysteresis; stability; recombination

1. Introduction

Our sun is an inexhaustible, enormous, clean, and free source of fuel. Acting as a natural nuclear reactor, the sun releases packets of energy known as photons to which an hour of photon exposure generates sufficient energy to quench the annual global energy thirst on Earth, theoretically [1]. Photovoltaic power from the sun is harnessed using solar cells made from semiconductors. When photons strike the surface of the solar cell, electrons from the valence band within the semiconductor material are excited to the conduction band. As charge carriers flow through the solar cell, an electric circuit is formed, successfully converting sunlight to useful electricity. Silicon semiconductor has been the primary material used in solar cells since the 1950s [2]. This is mostly because silicon is abundant, stable, with a favourable bandgap for solar absorption. However, manufacturing of crystalline silicon solar cells is tedious and energy-intensive to which numerous processes are required to transform the large ingot to a highly pure silicon wafer. In the last decade, scientists discovered the use of organic-inorganic halide perovskite (OIHP) materials as an effective light absorber for solar cell application. Due to the compositional flexibility of the perovskite material, band gap of the OIHP material can be easily tuned to match the sun's spectrum. In addition, OIHP solar cell can be manufactured at a much lower cost and required power. With current certified power conversion efficiency (PCE) at 25.2 % being comparable to that of well-established silicon solar cells, the suitability of OIHP materials for solar cell application is undeniable [3].

Endowed with properties such as direct band gaps, low exciton binding energies, high optical extinction coefficients, high charge mobilities, and long carrier diffusion lengths, perovskite materials also display balanced and ambipolar charge transport properties [4,5]. Under those circumstances, perovskite solar cells, theoretically, do not require any charge transport layer. Instead, the active perovskite absorber film permits direct transport of harvested charge carriers to their respective electrodes [5]. Such a device simplifies fabrication

procedure, reduces cost incurred from the use of expensive charge transport materials such as poly(3,4−ethylenedioxythiophene) polystyrene sulfonate (PEDOT:PSS), and improves stability commonly associated with detrimental reactions at the charge transport/perovskite interface. Unfortunately, power conversion efficiencies (PCEs) of devices without charge transport layers remain inferior [5,6].

Put simply, an ideal electron transport layer (ETL) extracts negatively charged carriers from the adjacent absorber film and transports them to the cathode. In essence, the ETL has two major roles. First, the presence of an ETL provides a cascading energy level such that electrons from the perovskite absorber are transported smoothly to the cathode with little charge accumulation [7,8]. Second, the ETL acts as a hole blocking layer, allowing unipolar transference while reducing carrier recombination tendencies [9]. As a result, widely reported electron transport materials are typically categorized into the following: (i) n-type metal oxide semiconductors such as titanium dioxide (TiO_2), zinc oxide (ZnO), tin (IV) oxide (SnO_2), tungsten (IV) oxide (WO_3), niobium pentoxide (Nb_2O_5) and zinc stannate (Zn_2SnO_4), (ii) n-type metal sulfide/selenide semiconductor such as cadmium selenide (CdSe), zinc sulfide (ZnS), and molybdenum disulfide (MoS_2), and (iii) n-type organic semiconductors such as [6,6]-phenyl-C_{61}-butyric acid methyl ester (PCBM), buckminsterfullerene (C60) and other fullerene derivatives [10].

While the laboratory performances of perovskite solar cells are rising rapidly, commercialization remains distant due to basic science and engineering challenges regarding the performance, hysteresis, reliability, and stability. Here, the importance and role of electron transport layers (ETLs) to the overall performance of OIHP solar cells are discussed. Effects of ETL on the quality of the perovskite film, charge transport, recombination, stability, and hysteresis of OIHP solar cells are emphasized. Recent developments on the device performance of OIHP solar cells with and without ETLs are also shown, displaying the

importance of ETL for high performing OIHP solar cells. In addition, designs of PSCs with different device configurations are discussed in brief. Hence, this review provides some guidance to improve device efficiency, stability, and hysteresis using rational ETL design.

2. ETL−free perovskite solar cells

A major advantage of the ETL-free perovskite solar cells is the ease of device fabrication since high temperatures utilized to crystallize metal oxide ETLs are omitted, along with the reduction in synthesis steps required. As such, the simplified device configuration found in ETL-free OIHP solar cells favours scalability and reduced manufacturing cost [11]. The performances of several ETL-free OIHP solar devices are listed in Fig.1. Early literatures featuring ETL-free OIHP solar cells were mostly created as control devices used primarily for comparison purposes against OIHP solar cells containing ETLs. Hence, initial photovoltaic parameters and stability of ETL-free OIHP devices were generally poor and undesirable [8,11]. Intentional ETL-free perovskite device was first fabricated by Liu et al. in 2014 whereby the ZnO-free solar device showed comparable results to the ZnO ETL solar device of 13.5 and 13.7 %, respectively [12]. The similar results were attributed to the increased series resistance in the ZnO ETL solar device but decreased surface recombination, vice versa. Shi et al. demonstrated superior stability in the ETL-free OIHP solar cell with device architecture of ITO/PEDOT:PSS/perovskite/Ti/Au [5]. The Ti layer, specified by the authors, does not act as an ETL but an interlayer to isolate the perovskite absorber layer and gold electrode. This is to ensure good interfacial contact while enhancing shunt resistance of the device. Remarkably, the ETL-free OIHP solar cell retained 70 % of initial PCE despite 300 h of storage under ambient conditions. That being said, the device showed inferior efficiency due to the low open−circuit voltage (V_{oc}) of 0.89, unlike the ETL based solar cell with V_{oc} close to 1 V. With the addition of the PCBM/C60 ETL, the OIHP solar cell attained PCE of 16.3 % while the ETL-free solar cell achieved lower PCE of 12.5 %.

Juarez-Perez et al. compared the photovoltaic parameters of OIHP solar cells with and without an ETL to which V_{OC} of device showed minor dependence while short-circuit current density (J_{sc}) and fill factor (FF) were drastically reduced in the absence of the ETL [13]. Although series resistance was increased with the addition of the electron transport material, recombination resistance improved tremendously, explaining the improved efficiency in the device containing the ETL. Furthermore, ETL-free OIHP solar devices showed unstable power output despite respectable PCE during J-V measurements [6,14]. In 2019, Huang fabricated ETL-free perovskite solar cells with champion device achieving PCE of 20.1 % [15]. The high efficiency attained, however, was drastically motivated by the employment of tetramethylammonium hydroxide (TMAH) molecules between the FTO electrode/perovskite interface to which the pristine device without TMAH showed inferior PCE of 14.4 %. The authors explained that addition of TMAH improved charge extraction and reduced recombination, suggesting the importance efficient charge transport at the cathode/perovskite interface. Hence, the use of ETL in OIHP solar cells still dominant in terms of efficiency and device stability.

3. Various device architectures

The attractiveness of the OIHP material as an effective photovoltaic absorber was obscure in the beginning. Back in 2009, organic-inorganic halide perovskite material was initially employed as a dye in dye-sensitized solar cell (DSSC) [16]. However, the incompatibility of the perovskite material with the liquid electrolyte led to low PCE of 3.8 % and fast device degradation. Replacement of the liquid electrolyte with the solid spiro−OMeTAD electrolyte by Kim et al. in 2012 allured several solar enthusiasts due to the rapid increase in device efficiency to 9.7 % and elongated lifetime of 500 h under continuous illumination [17]. As such, initial perovskite solar cells adopted the mesoscopic structure to which the electron transport layers were mesoporous since they mimicked the transport layers

of DSSCs. However, the mesoporous ETL structures are dissimilar. In DSSC, a thick mesoporous ETL is required to facilitate high dye loading with typical thickness of 10 µm [7,8]. On the contrary, an approximate thickness of 200 nm is sufficient to generate similar photocurrent in the OIHP solar cell [7]. As a matter of fact, the mesoporous structure is optional in an OIHP solar cell although the large surface area provided aids in electron extraction. The compact ETL has proven to be more important since it prevents charge recombination between the FTO/perovskite interface and charge leakage. In 2012, Snaith et al. proposed the use of the planar structure whereby the mesoscopic structure was discarded and only the compact ETL was employed [18]. Unlike the mesoporous counterpart which requires complicated fabrication steps, the planar ETL structure is straightforward with clear advantage for large-scale manufacturing. However, attained PCE was low of 1.8 % owing to the poor perovskite film coverage and shunting issues. In 2013, Liu et al improved the film coverage of the perovskite film by using vapour deposition over the compact-TiO_2 (c-TiO_2) layer and attained PCE of 15 % [19]. Depending on the position of the charge transport layers, specifically the ETL and hole transport layer (HTL), the device architecture can be further split into regular or inverted. In the regular (n-i-p) perovskite solar cell, the ETL is placed between the cathode and OIHP layers. In the inverted (p-i-n) architecture, the ETL is between OIHP absorber and the cathode. Fig. 2a illustrates the 4 main device architectures employed in OIHP solar cells namely, mesoporous n-i-p, mesoporous p-i-n, planar n-i-p, and planar p-i-n. As seen in Fig. 2b, the charge transport layers provide smooth injection and transport of selective charge carriers [8].

4. The roles of ETL

To achieve high performance of PSCs, ETLs should fulfil a list of criteria [7,10]. First, the lowest unoccupied molecular orbital (LUMO) of the conduction band in the ETL should be comparable or slightly lower compared to the adjacent OIHP layer. Preferably, the ETL should possess LUMO level in-between that of the OIHP perovskite layer and the electron

collecting electrode, ensuring smooth electron transference. Second, the highest occupied molecular orbital (HOMO) of the valence band in the ETL should be deep such that hole transference across the ETL/perovskite interface is deprived, reducing the occurrence of charge recombination. Third, the ETL should have high transparency, uniform film morphology, and suitable energy level. The strong electron-accepting property further facilitates electron extraction which explains the frequent use of materials with high electron affinity and ion potential.

In the n-i-p structure, the ETL should also have a wide band gap with little absorbance in the visible wavelengths to reduce optical energy losses. The ETL should also have good antireflection quality to avoid scattering and reflection of light. In addition, the compact ETL should not have pinholes so as to prevent charge current leakage. For the mesoporous structure, the ETL should have sufficient porosity to encourage easy infiltration of the perovskite material. It is important to ensure complete filling of the perovskite material to prevent direct contact with the HTL which could result in low shunt resistance. Moreover, existence of voids within the mesoporous ETL could contain air whereby the presence of free oxygen molecules could increase decomposition of the perovskite material, lowering the stability of the OIHP solar cell [7]. Given these points, an ideal ETL ensures high quality perovskite morphology, efficient electron transportation, lowers recombination tendencies and charge accumulation, indirectly reducing the hysteresis effect while improving device stability.

5. Quality of perovskite film

One of the most significant factors influencing the overall performance of a perovskite solar cell is the quality of the OIHP absorber layer [2-5]. Over the past few years, large efforts have been placed into the optimization of the morphology and quality of the perovskite film. Various methods such as hot casting, antisolvent, solvent annealing, and ETL engineering have been tested [2,3]. Since the OIHP film is usually fabricated directly on top of the ETL in an

n-i-p structure, quality of the absorber film is highly dependent on the morphology, roughness, and interfacial contact with the underlying electron transport film. Favourable chemical interaction between the terminating groups of the electron transport material with the OIHP material also influence the nucleating and crystallization processes of the perovskite film [8,10]. In addition, the surface energy of the ETL affects the wetting properties of the perovskite solution, crucial to the crystallization, grain size, density of grain boundaries of the OIHP film.

To illustrate, Ogomi et al. deposited a thin layer of HOCO-R-$NH_3^+I^-$ on the surface of the meso-Al_2O_3 layer before using the two-step approach to fabricate the methylammonium lead iodide ($MAPbI_3$) absorber layer [20]. In the presence of the HOCO−R−$NH_3^+I^-$ layer, growth of the lead iodide (PbI_2) network was enhanced whereby full coverage was observed. The authors attributed the improved perovskite quality to the superior miscibility between the $NH_3^+I^-$ terminating group and the PbI_2 crystals. X-ray diffraction patterns of PbI_2 crystal structure without the HOCO-R-$NH_3^+I^-$ layer showed similar peaks to the commercially available PbI_2 powder. On the other hand, the x-ray pattern of the ETL modified sample showed only [001] and [003] peaks, implying significant control over the growth direction of the adjacent PbI_2 film. Yang et al. also exhibited the significance of ETL engineering in improving the surface morphology of the adjacent OIHP film [21].

6. Charge Transport and Recombination

Charge mobility and energy level alignment of the ETL are crucial to the charge transport and recombination of the solar device. In general, ETLs with high electron affinity and ion potential improve extraction efficiency of photogenerated electrons from the OIHP film and transportation to the cathode [22]. By possessing comparable or slightly lower lowest unoccupied molecular orbital (LUMO) along with a much deeper highest occupied molecular orbital (HOMO) compared to the perovskite film, efficient transport of electrons is encouraged while transportation of holes is discouraged. Such favourable energy level alignments at the

ETL/perovskite interface strengthen selective electron transport, reduce charge accumulation, and decrease recombination susceptibility [10,22]. In addition, electron transport materials with low conductivity or electron mobility lead to increased series resistance. With impeded charge transportation at the ETL/perovskite interface, charge accumulation increases, resulting in higher tendencies for recombination at the interface. Attained FF and V_{oc} during current density-voltage (J-V) measurement is often used as indicators to the series conductivity and recombination resistance of the device [8]. Table 1. summarizes various champion ETL based solar devices with their corresponding V_{oc}, FF, and PCE.

TiO_2 material shows inferior electron mobility of 0.1−4.0 $cm^2\ V^{-1}\ s^{-1}$ [23,24]. To overcome the low mobility TiO_2 ETL, three strategies are commonly utilized. The first approach is to utilize a different electron transport material with superior intrinsic optoelectronics properties. For instance, the mobility of SnO_2 and ZnO show 240 and 205−300 $cm^2\ V^{-1}\ s^{-1}$ [24]. Anaraki et al. obtained an efficiency of 21 % using the SnO_2 based device [25]. The second approach is to modify the ETL using dopants. For example, Yang et al. reported that the mobility of SnO_2 and EDTA-doped SnO_2 film are 9.92×10^{-4} and 2.27×10^{-3} $cm^2\ V^{-1}\ s^{-1}$[26]. When small YCl_3 was added to the TiO_2 film, increased energy level from -4.08 to -3.95 eV was observed [26]. Well-matched energy level alignment and shortened time-resolved photoluminescent (trPL) decay lifetime from 14.16 to 0.97 ns were also observed when the EDTA dopant was utilized. In the absence of EDTA, the pristine device attained low PCE of 16.42 % while the EDTA doped SnO_2 ETL device attained superior efficiency of 21.06 %. Last but not least, the surface of ETLs can be enhanced through the use of a thin interlayer between the ETL/perovskite interface [7,10,22]. Zhu et al. utilized graphene quantum dots (GQDs) as an electron bridge, facilitating electron injection between the $MAPbI_3$ and TiO_2 ETL [27]. Therefore, the ETL is pivotal to the efficiency of electron transportation and recombination resistance of the OIHP solar cell.

7. Hysteresis

Several mechanisms have been proposed to explain the hysteresis phenomenon observed in J-V curves. These mechanisms include ferroelectricity in the perovskite film, charge accumulation at the electrodes, ion migration within the OIHP layer, and charge trapping/detrapping processes [28]. Depending on factors such as prebias, scan rate, direction, and voltage range, photovoltaic parameters attained vary drastically, reducing the reliability and accuracy of the device performance. In recent years, ion migration has garnered great support as the main cause for hysteresis [29−32]. During applied bias, ions within the perovskite film migrate towards their respective electrodes, accumulating at the interfaces while leaving behind the oppositely charged carriers. Due to the small activation energy found in halide vacancies, Walsh et al. proposed that migration of halide vacancies within the OIHP layer causes ion migration [29]. This was further supported by Luo et al. to which halide migration was observed in perovskite single crystals [30]. Yuan et al. also noticed migration of iodide ions under electrical pooling at 330 K [31]. However, migration of ions within the OIHP films does not explain the importance of charge transport layers on the degree of hysteresis, as seen experimentally. Fig. 3 illustrates the importance of ETL optimization in hysteresis-free perovskite solar devices. Yu et al. showed that the degree of hysteresis is larger in the ETL-free perovskite device compared to the TiO_2 ETL solar device [33]. Heo et al. further showed negligible hysteresis when the ETL employed was [6,6]–phenyl–C61–butyric acid methyl ester (PCBM) instead of TiO_2 [34]. Shao et al. explained that the PCBM ETL could reduce the amount of surface traps found at the perovskite/ETL interface, reducing the extent of hysteresis [35].

By lowering the density of trap states found within the bulk electron transport material and surface of the ETL, ETL engineering is often seen as a facile approach to reduce the degree of hysteresis. To illustrate, Peng et al. modified the meso-TiO_2 ETL by depositing a thin layer

of PMMA:PCBM on the surface, resulting in negligible hysteresis even during J-V measurements conducted at different scan rates [36]. The authors attributed the absence of hysteresis to the passivation of trap states at the TiO_2/OIHP interface, to which the reduced trapped carriers allowed faster transient response. Woiciechowski et al. functionalized the c−TiO_2 ETL by immersing the substrate in a solution of fullerene self-assembled monolayer (C60−SAM), to form the C60−SAM modified c-TiO_2 ETL [37]. At all employed scan rates, the modified ETL solar cell showed much smaller hysteresis compared to the pristine device. The authors ascribed the improved hysteresis to the reduced surface recombination and enhanced charge extraction. Another approach to reduce hysteresis in OIHP solar cells is to dope the underlying ETL film. For example, Luan et al. attributed the negligible hysteresis in the 2,2,2−trifluoroethanol doped SnO_2 ETL OIHP solar cell to the improved mobility and reduced defects of the doped ETL [38]. Yang et al. also showed similar trend to which the yttrium doped SnO_2 (Y-SnO_2) ETL OIHP solar cell showed significantly lower degree of hysteresis compared to the undoped SnO_2 device [39]. Photoluminescence results revealed superior PL quenching in the glass/Y-SnO_2/$MAPbI_3$ sample compared to the glass/SnO_2/$MAPbI_3$, signifying enhanced charge extraction across the ETL/perovskite interface, reducing the accumulation of capacitive charges. Hence, it is vital to employ a suitable ETL to minimize possible hysteresis in the perovskite solar device.

8. Stability

Organic-inorganic halide perovskite material is highly sensitive to multiple factors namely, moisture, temperature, oxygen, illumination, and UV exposure [9,11]. During device preparation and testing, the perovskite solar device is often exposed to such stresses, unintentionally degrading the absorber layer. Shaikh et al. and Mahmood et al. explained that $MAPbI_3$, when exposed to humidity, breakdowns into methylammonium iodide (MAI) and PbI_2 molecules, which further degrades into hydrogen iodide (HI), PbI_2, and methylamine

(MA) constituents [40,41]. This is because OIHP is hydrophilic and readily absorbs water. In the p-i-n structure, employment of a hydrophobic ETL layer allows moisture protection by preventing water molecules from penetrating to the underlying film. For example, Shao et al. utilized various n-type polymers as the electron transport material and showed superior ambient stability whereby the device retained 87 % of initial PCE despite exposure to air for 270 mins [42]. On the other hand, the PCBM ETL OIHP solar cell showed significant decay in initial PCE value to 3.5 %. Optical micrographs further revealed severe changes to the underlying perovskite film in the PCBM ETL OIHP device whereby large MAI grains with diameter greater than 1 mm were observed. On the contrary, perovskite film in the n-type polymer ETL OIHP device showed little morphological change. Unlike the n-type polymer ETL which acted as an effective encapsulation layer, the hydrophilic PCBM ETL encouraged moisture diffusion to the perovskite layer, eventually degrading the perovskite film to produce the methylammonium iodide constituent.

The use of unfavourable ETL can also accelerate degradation in an unencapsulated OIHP solar cell when exposed to light and oxygen. Bryant et al. revealed that degradation of the $MAPbI_3$ film can be slowed down by removing electrons from the OIHP film before possible reaction with oxygen [39]. As such, by using an ETL with enhanced electron extraction capabilities, photostability of OIHP solar cells can be significantly enhanced. In addition, the properties of the electron transport material play important roles in the overall stability of the device. For example, ZnO is chemically instable, PEDOT:PSS is highly hydroscopic, and TiO_2 is unstable under UV illumination [9,11,44]. To illustrate, TiO_2 is as a photocatalytic material and contains large density of oxygen vacancies. Presence of oxygen vacancies serve as deep electron donating sites, encouraging oxygen absorption from the atmosphere, acting as trap sites near the conduction band edge [45−47]. Under UV illumination, Ito et al. further proposed that holes could be generated within the TiO_2 ETL, promoting electron extraction from the I^- anion found

in the perovskite film, degrading the absorber film [47]. As reported by Li et.al., the bis(formato)dimethyltin(IV) ETL with potassium chloride treated based perovskite device shows better photovoltaic performance (22.21 %) and long term-stability (130 days) than the traditional SnO_2 based perovskite solar cell device [47]. The poly methyl methacrylate (PMMA) layer introduced in perovskite/HTL interface, which can protect the perovskite film from moisture and oxygen erosion. The unsealed device still retains 95% of the initial PCE under ambient conditions with 60% relative humidity for 30 days [47].

As seen in Fig. 4, several research groups used alternative electron transport materials as well as sensible dopants to overcome possible degradation implications. To demonstrate, Leijtens et al. showed stable photocurrent for over 1000 h in the meso-Al_2O_3 ETL OIHP solar cell when exposed to 76.5 mW cm^{-2} UV-light illumination at 40 °C [45]. In contrast, the TiO_2 ETL OIHP solar cell degraded within 3 h. In 2017, Tan et al. used chlorine doped TiO_2 film and retained 90 % of initial efficiency despite 500 h [48].

9. Conclusion

Immense efforts placed into the development of perovskite solar cells continue to reveal promising qualities of perovskite materials as highly efficient photovoltaic harvesters. Unfortunately, commercialization of OIHP solar cells is greatly hampered by issues such as poor charge transport, recombination, hysteresis, and device instability. In this paper, the importance and progress of ETLs are briefly explored. The use of rational ETLs favour improved efficiency, hysteresis, and stability in perovskite solar cells through tailored energy levels, reduced defect densities, and enhanced charge transportation. In essence, this work shows the prominence of employing an appropriate ETL to improve the overall performance of OIHP solar devices.

For an efficient perovskite solar cells, the ETL should have high electrical conductivity, good optical transparency, uniform film morphology, suitable energy level, high electron mobility, charge transfer/blocking holes, and low cost. But, to boost the efficiency and stability of ETL materials for perovskite devices, some new strategies and challenges continue to require further considered. In the future, developing simple low temperature processing route, device structure, doping concentration, optimization of scaffold thickness, new organic ETL, and perovskite composition will be a promising direction and trend. Scientistic are putting their continuous efforts to overcome the challenges and towards the development of PSCs with improved stability and PCE.

Conflict of Interest

There are no conflicts to declare.

Acknowledgment

The research is supported by AcRF Tier2 grant (MOE-T2EP50121-0012) from Singapore Ministry of Education

References

1. Kim JY, Lee JW, Jung HS, Shin H, Park NG. High-efficiency perovskite solar cells. Chemical Reviews. 2020;120:7867-918.
2. Miles RW, Hynes KM, Forbes I. Photovoltaic solar cells: An overview of state-of-the-art cell development and environmental issues. Progress in crystal growth and characterization of materials. 2005;51:1-42.
3. NREL, Best Research-Cell Efficiency Chart, (n.d.).https://www.nrel.gov/pv/assets/images/ efficiency-chart.png (accessed May 28, 2020).
4. Feng J, Xiao B. Effective masses and electronic and optical properties of nontoxic $MASnX_3$ (X= Cl, Br, and I) perovskite structures as solar cell absorber: a theoretical study using HSE06. *J Phys Chem. C.* 2014;118:19655-19660.
5. Shi T, Chen J, Zheng J, Li X, Zhou B, Cao H, Wang Y. Ti/Au Cathode for Electronic transport material-free organic-inorganic hybrid perovskite solar cells. *Sci Rep.* 2016;6:39132.
6. Zhang Y, Liu M, Eperon GE, Leijtens TC, McMeekin D, Saliba M, Zhang W, de Bastiani M, Petrozza A, Herz LM, Johnston MB. Charge selective contacts, mobile ions and anomalous hysteresis in organic–inorganic perovskite solar cells. *Mater Horiz.* 2015;2:315-22.
7. Noh MF, Teh CH, Daik R, Lim EL, Yap CC, Ibrahim MA, Ludin NA, bin Mohd Yusoff AR, Jang J, Teridi MA. The architecture of the electron transport layer for a perovskite solar cell. *J Mater Chem C.* 2018;6:682-712; Thambidurai M, Febriansyah B, Foo S, Harikesh PC, Ming KT, Mathews N, Dang C. Enhanced stability and photovoltaic performance of planar perovskite solar cells through anilinium thiobenzoate interfacial engineering. *J. Power Sources.* 2020;479:228811; Sakthivel P, Foo S, Thambidurai M,

Harikesh PC, Mathews N, Yuvakkumar R, Ravi G, Dang C. Efficient and stable planar perovskite solar cells using co-doped tin oxide as the electron transport layer. *J Power Sources.* 30;471:228443.

8. Yang G, Tao H, Qin P, Ke W, Fang G. Recent progress in electron transport layers for efficient perovskite solar cells. *J Mater Chem A.* 2016;4:3970-3990; Foo S, Thambidurai M, Harikesh PC, Mathews N, Huang Y, Dang C. Interfacial 2-hydrozybenzophenone passivation for highly efficient and stable perovskite solar cells. *J Power Sources.* 2020;475:228665; Thambidurai M, Shini F, Kim JY, Lee C, Dang C. Solution-processed Ga-TiO2 electron transport layer for efficient inverted organic solar cells. *Mater Lett.* 2020;274:128003.
9. Mahmood K, Sarwar S, Mehran MT. Current status of electron transport layers in perovskite solar cells: materials and properties. *RSC Adv*. 2017;7:17044–17062.
10. Wang K, Olthof S, Subhani WS, Jiang X, Cao Y, Duan L, Wang H, Du M, Liu SF. Novel inorganic electron transport layers for planar perovskite solar cells: Progress and prospective. *Nano Energy*. 2020;68:104289.
11. Huang L, Ge Z. Simple, Robust, and Going More Efficient: Recent Advance on Electron Transport Layer-Free Perovskite Solar Cells. *Adv Energy Mater.* 2019;9:1900248.
12. Liu D, Yang J, Kelly TL. Compact layer free perovskite solar cells with 13.5% efficiency. *J Am Chem Soc*. 2014;136:17116-22.
13. Juarez-Perez EJ, Wubler M, Fabregat-Santiago F, Lakus-Wollny K, Mankel E, Mayer T, Jaegermann W, Mora-Sero I. Role of the selective contacts in the performance of lead halide perovskite solar cells. *J Phys Chem Lett.* 2014;5:680-685.
14. Fu Q, Tang X, Huang B, Hu T, Tan L, Chen L, Chen Y. Recent progress on the long-term stability of perovskite solar cells. *Adv. Sci*. 2018;5:1700387.

15. Huang C, Lin P, Fu N, Liu C, Xu B, Sun K, Wang D, Zeng X, Ke S. Facile fabrication of highly efficient ETL-free perovskite solar cells with 20% efficiency by defect passivation and interface engineering. *ChemComm.* 2019;55:2777-2780.
16. Kojima A, Teshima K, Shirai Y, Miyasaka T. Organometal halide perovskites as visible-light sensitizers for photovoltaic cells. *J Am Chem* Soc. 2009;131:6050-6051.
17. Kim HS, Lee CR, Im JH, Lee KB, Moehl T, Marchioro A, Moon SJ, Humphry-Baker R, Yum JH, Moser JE, Grätzel M. Lead iodide perovskite sensitized all-solid-state submicron thin film mesoscopic solar cell with efficiency exceeding 9%. *Sci Rep.* 2012;2:591.
18. Lee MM, Teuscher J, Miyasaka T, Murakami TN, Snaith HJ. Efficient hybrid solar cells based on meso-superstructured organometal halide perovskites. Science. 2012;338:643-647.
19. Liu M, Johnston MB, Snaith HJ. Efficient planar heterojunction perovskite solar cells by vapour deposition. *Nature.* 2013;501:395-398.
20. Ogomi Y, Morita A, Tsukamoto S, Saitho T, Shen Q, Toyoda T, Yoshino K, Pandey SS, Ma T, Hayase S. All-solid perovskite solar cells with HOCO-R-$NH3^{+}I^{-}$anchor-group inserted between porous titania and perovskite. *J Phys Chem.* 2014;118:16651-16659.
21. Yang G, Wang C, Lei H, Zheng X, Qin P, Xiong L, Zhao X, Yan Y, Fang G. Interface engineering in planar perovskite solar cells: energy level alignment, perovskite morphology control and high-performance achievement. *J Mater Chem A.* 2017;5:1658-66.
22. Shao S, Loi MA. The role of the interfaces in perovskite solar cells. *Adv Mater Interfaces.* 2020;7:1901469.

23. Zhang P, Wu J, Zhang T, Wang Y, Liu D, Chen H, Ji L, Liu C, Ahmad W, Chen ZD, Li S. Perovskite solar cells with ZnO electron-transporting materials. *Adv Mater.* 2018;30:1703737; Thambidurai M, Shini F, Harikesh PC, Mathews N, Dang C. Highly stable and efficient planar perovskite solar cells using ternary metal oxide electron transport layers. *J Power Sources.* 2020;448:227362; Shini F, Thambidurai M, Harikesh PC, Mathews N, Huang Y, Dang C. Heterogeneous electron transporting layer for reproducible, efficient and stable planar perovskite solar cells. J Power Sources. 2019;437:226907; Thambidurai M, Foo S, Salim KM, Harikesh PC, Bruno A, Jamaludin NF, Lie S, Mathews N, Dang C. Improved photovoltaic performance of triple-cation mixed-halide perovskite solar cells with binary trivalent metals incorporated into the titanium dioxide electron transport layer. *J Mater Chem C.* 2019;7:5028-5036.

24. Chen Y, Meng Q, Zhang L, Han C, Gao H, Zhang Y, Yan H. SnO2-based electron transporting layer materials for perovskite solar cells: A review of recent progress. *J Energy Chem.* 2019;35:144-67.

25. Anaraki EH, Kermanpur A, Steier L, Domanski K, Matsui T, Tress W, Saliba M, Abate A, Grätzel M, Hagfeldt A, Correa-Baena JP. Highly efficient and stable planar perovskite solar cells by solution-processed tin oxide. *Energy Environ Sci.* 2016;9:3128-3134.

26. Yang D, Yang R, Wang K, Wu C, Zhu X, Feng J, Ren X, Fang G, Priya S, Liu SF. High efficiency planar-type perovskite solar cells with negligible hysteresis using EDTA-complexed SnO_2. *Nat Comm.* 2018;9:3239; *RSC Advances.* 2014;4:9652-9655; Li M, Huan Y, Yan X, Kang Z, Guo Y, Li Y, Liao X, Zhang R, Zhang Y. Efficient Yttrium (III) Chloride-Treated TiO_2 Electron Transfer Layers for Performance-

Improved and Hysteresis-Less Perovskite Solar Cells. *ChemSusChem*. 2018;11:171-177.

27. Zhu Z, Ma J, Wang Z, Mu C, Fan Z, Du L, Bai Y, Fan L, Yan H, Phillips DL, Yang S. Efficiency enhancement of perovskite solar cells through fast electron extraction: the role of graphene quantum dots. J Am Chem Soc. 2014;136:3760-3763.
28. Kang DH, Park NG. On the current–voltage hysteresis in perovskite solar cells: dependence on perovskite composition and methods to remove hysteresis. Adv Mater. 2019;31:1805214.
29. Walsh A, Scanlon DO, Chen S, Gong XG, Wei SH. Self-regulation mechanism for charged point defects in hybrid halide perovskites. *Angew Chem. Int Ed*. 2015;127:1811-4.
30. Luo Y, Khoram P, Brittman S, Zhu Z, Lai B, Ong SP, Garnett EC, Fenning DP. Direct observation of halide migration and its effect on the photoluminescence of methylammonium lead bromide perovskite single crystals. *Adv Mater.* 2017;29:1703451.
31. Yuan Y, Wang Q, Shao Y, Lu H, Li T, Gruverman A, Huang J. Electric-field-driven reversible conversion between Methylammonium lead triiodide perovskites and lead iodide at elevated temperatures. *Adv Energy Mater*. 2016;6:1501803.
32. Lee H, Gaiaschi S, Chapon P, Marronnier A, Lee H, Vanel JC, Tondelier D, Boureé JE, Bonnassieux Y, Geffroy B. Direct Experimental Evidence of Halide Ionic Migration under Bias in CH3NH3PbI$_{3-x}$ Cl$_x$ Based Perovskite Solar Cells Using GD-OES Analysis. *ACS Energy Lett.* 2017;2:943-9.
33. Yu H, Ryu J, Lee JW, Roh J, Lee K, Yun J, Lee J, Kim YK, Hwang D, Kang J, Kim SK. Large grain-based hole-blocking layer-free planar-type perovskite solar cell with best efficiency of 18.20%. *ACS appl Mater interfaces.* 2017;9:8113-8120.

34. Heo JH, Han HJ, Kim D, Ahn TK, Im SH. Hysteresis-less inverted CH3NH3PbI3 planar perovskite hybrid solar cells with 18.1% power conversion efficiency. *Energy Environ Sci.* 2015;8:1602-8.

35. Shao Y, Xiao Z, Bi C, Yuan Y, Huang J. Origin and elimination of photocurrent hysteresis by fullerene passivation in $CH_3NH_3PbI_3$ planar heterojunction solar cells. *Nat Commun.* 2014;5:5784.

36. Peng J, Wu Y, Ye W, Jacobs DA, Shen H, Fu X, Wan Y, Wu N, Barugkin C, Nguyen HT, Zhong D. Interface passivation using ultrathin polymer–fullerene films for high-efficiency perovskite solar cells with negligible hysteresis. *Energy Environ Sci.* 2017;10:1792-800.

37. Wojciechowski K, Leijtens T, Siprova S, Schlueter C, Hörantner MT, Wang JT, Li CZ, Jen AK, Lee TL, Snaith HJ. C_{60} as an efficient n-type compact layer in perovskite solar cells. *J. Phys Chem Lett.* 2015;6:2399-2405.

38. Luan Y, Yi X, Mao P, Wei Y, Zhuang J, Chen N, Lin T, Li C, Wang J. High-performance planar perovskite solar cells with negligible hysteresis using 2, 2, 2-trifluoroethanol-incorporated SnO2. *IScience*. 2019;16:433-441.

39. Yang G, Lei H, Tao H, Zheng X, Ma J, Liu Q, Ke W, Chen Z, Xiong L, Qin P, Chen Z. Reducing hysteresis and enhancing performance of perovskite solar cells using low-temperature processed Y-doped SnO_2 nanosheets as electron selective layers. *Small.* 2017;13:1601769.

40. Shaikh JS, Shaikh NS, Sheikh AD, Mali SS, Kale AJ, Kanjanaboos P, Hong CK, Kim JH, Patil PS. Perovskite solar cells: In pursuit of efficiency and stability. *Mater Des.* 2017;136:54-80.

41. Mahmood K, Sarwar S, Mehran MT. Current status of electron transport layers in perovskite solar cells: materials and properties. *Rsc Advances.* 2017;7:17044-17062.

42. Shao S, Chen Z, Fang HH, Ten Brink GH, Bartesaghi D, Adjokatse S, Koster LJ, Kooi BJ, Facchetti A, Loi MA. N-type polymers as electron extraction layers in hybrid perovskite solar cells with improved ambient stability. J Mater Chem A. 2016;4:2419-2426.
43. Bryant D, Aristidou N, Pont S, Sanchez-Molina I, Chotchunangatchaval T, Wheeler S, Durrant JR, Haque SA. Light and oxygen induced degradation limits the operational stability of methylammonium lead triiodide perovskite solar cells. *Energy Environ Science.* 2016;9:1655-1660.
44. Roy P, Sinha NK, Tiwari S, Khare A. A review on perovskite solar cells: Evolution of architecture, fabrication techniques, commercialization issues and status. *Sol Energy.* 2020;198:665-88.
45. Leijtens T, Eperon GE, Pathak S, Abate A, Lee MM, Snaith HJ. Overcoming ultraviolet light instability of sensitized TiO_2 with meso-superstructured organometal tri-halide perovskite solar cells. *Nat Commun.* 2013;4(1):2885.
46. Nakamura I, Negishi N, Kutsuna S, Ihara T, Sugihara S, Takeuchi K. Role of oxygen vacancy in the plasma-treated TiO2 photocatalyst with visible light activity for NO removal. *J Mol Cata A: Chem.* 2000;161:205-212.
47. Ito S, Tanaka S, Manabe K, Nishino H. Effects of surface blocking layer of Sb_2S_3 on nanocrystalline TiO_2 for $CH_3NH_3PbI_3$ perovskite solar cells. *J Phys Chem C.* 2014;118:16995-7000; Li F, Shen Z, Weng Y, Lou Q, Chen C, Shen L, Guo W, Li G. Novel Electron Transport Layer Material for Perovskite Solar Cells with Over 22% Efficiency and Long-Term Stability. Adv Funct Mater. 2020;30:2004933; Liu P, Liu Z, Qin C, He T, Li B, Ma L, Shaheen K, Yang J, Yang H, Liu H, Liu K. High-performance perovskite solar cells based on passivating interfacial and intergranular defects. Sol Energy Mater Sol Cells. 2020;212:110555.

48. Tan H, Jain A, Voznyy O, Lan X, De Arquer FP, Fan JZ, Quintero-Bermudez R, Yuan M, Zhang B, Zhao Y, Fan F. Efficient and stable solution-processed planar perovskite solar cells via contact passivation. *Science.* 2017;355:722-726.
49. Hu Q, Wu J, Jiang C, Liu T, Que X, Zhu R, Gong Q. Engineering of electron-selective contact for perovskite solar cells with efficiency exceeding 15%. *ACS Nano.* 2014;8:10161-10167.
50. Zheng L, Ma Y, Wang Y, Xiao L, Zhang F, Yang H. Hole blocking layer-free perovskite solar cells with over 15% efficiency. *Energy Procedia.* 2017;105:188-193.
51. Topolovsek P, Lamberti F, Gatti T, Cito A, Ball JM, Menna E, Gadermaier C, Petrozza A. Functionalization of transparent conductive oxide electrode for TiO_2-free perovskite solar cells. *J Mater Chem A.* 2017;5:11882-11893.
52. Zhao P, Han M, Yin W, Zhao X, Kim SG, Yan Y, Kim M, Song YJ, Park NG, Jung HS. Insulated interlayer for efficient and photostable electron-transport-layer-free perovskite solar cells. *ACS Appl Mater interfaces.* 2018;10:10132-10140.
53. Xu X, Chen Q, Hong Z, Zhou H, Liu Z, Chang WH, Sun P, Chen H, Marco ND, Wang M, Yang Y. Working mechanism for flexible perovskite solar cells with simplified architecture. *Nano lett*. 2015;15:6514-6520.
54. Cui P, Wei D, Ji J, Song D, Li Y, Liu X, Huang J, Wang T, You J, Li M. Highly efficient electron-selective layer free perovskite solar cells by constructing effective p–n heterojunction. *Solar RRL*. 2017;1:1600027.
55. Liao JF, Wu WQ, Jiang Y, Kuang DB, Wang L. Maze-Like Halide Perovskite Films for Efficient Electron Transport Layer-Free Perovskite Solar Cells. *Solar RRL*. 2019;3:1800268.

56. Han Q, Ding J, Bai Y, Li T, Ma JY, Chen YX, Zhou Y, Liu J, Ge QQ, Chen J, Glass JT. Carrier dynamics engineering for high-performance electron-transport-layer-free perovskite photovoltaics. *Chem.* 2018;4:2405-2417.
57. Tang Y, Roy R, Zhang Z, Hu Y, Yang F, Qin C, et al. Rubidium chloride doping TiO_2 for efficient and hysteresis-free perovskite solar cells with decreasing traps. Sol Energy. 2022;231:440–446.
58. Sanehira Y, Shibayama N, Numata Y, Ikegami M, Miyasaka T. Low-Temperature Synthesized Nb-Doped TiO_2 Electron Transport Layer Enabling High-Efficiency Perovskite Solar Cells by Band Alignment Tuning. ACS Appl Mater Interfaces. 2020;12:15175–15182.
59. Tan H, Jain A, Voznyy O, Lan X, De Arquer FPG, Fan JZ, et al. Efficient and stable solution-processed planar perovskite solar cells via contact passivation. Science. 2017;355:722–726.
60. Gong X, Sun Q, Liu S, Liao P, Shen Y, Grätzel C, Zakeeruddin SM, Grätzel M, Wang M. Highly efficient perovskite solar cells with gradient bilayer electron transport materials. Nano lett. 2018;18:3969-3977.
61. Xie J, Huang K, Yu X, Yang Z, Xiao K, Qiang Y, Zhu X, Xu L, Wang P, Cui C, Yang D. Enhanced electronic properties of SnO_2 via electron transfer from graphene quantum dots for efficient perovskite solar cells. *Acs Nano.* 2017;11:9176-9182.
62. Subbiah AS, Mathews N, Mhaisalkar S, Sarkar SK. Novel Plasma-assisted low-temperature-processed SnO_2 thin films for efficient flexible perovskite photovoltaics. *ACS Energy Lett.* 2018;3:1482-1491
63. Guo Q, Wu J, Yang Y, Liu X, Lan Z, Lin J, Huang M, Wei Y, Dong J, Jia J, Huang Y. High-performance and hysteresis-free perovskite solar cells based on rare-earth-doped SnO2 mesoporous scaffold. *Research*. 2019:1-13.

64. Chen J, Zhao X, Kim SG, Park NG. Multifunctional chemical linker imidazoleacetic acid hydrochloride for 21% efficient and stable planar perovskite solar cells. Adv Mater. 2019;31:1902902.

65. Yang D, Yang R, Wang K, Wu C, Zhu X, Feng J, et al. High efficiency planar-type perovskite solar cells with negligible hysteresis using EDTA-complexed SnO_2. Nat Commun. 2018;9:3239.

66. You Y, Tian W, Min L, Cao F, Deng K, Li L. TiO_2/WO_3 bilayer as electron transport layer for efficient planar perovskite solar cell with efficiency exceeding 20%. *Adv Mater Interfaces.* 2020;7:1901406.

67. Zhao X, Liu S, Zhang H, Chang SY, Huang W, Zhu B, Shen Y, Shen C, Wang D, Yang Y, Wang M. 20% efficient perovskite solar cells with 2D electron transporting layer. *Adv Funct Mater.* 2019;29:1805168.

68. Wang Z, Lou J, Zheng X, Zhang WH, Qin Y. Solution processed Nb2O5 electrodes for high efficient ultraviolet light stable planar perovskite solar cells. ACS Sustain Chem Eng. 2019;7:7421-7429.

69. Zheng X, Chen B, Dai J, Fang Y, Bai Y, Lin Y, Wei H, Zeng XC, Huang J. Defect passivation in hybrid perovskite solar cells using quaternary ammonium halide anions and cations. *Nat Energy*. 2017;2:17102.

70. Shin SS, Yeom EJ, Yang WS, Hur S, Kim MG, Im J, Seo J, Noh JH, Seok SI. Colloidally prepared La-doped $BaSnO_3$ electrodes for efficient, photostable perovskite solar cells. *Science.* 2017;356:167-71

71. Tavakoli MM, Yadav P, Tavakoli R, Kong J. Surface engineering of TiO2 ETL for highly efficient and hysteresis-less planar perovskite solar cell (21.4%) with enhanced open-circuit voltage and stability. *Adv Energy Mater*. 2018;8:1800794.

72. Chen R, Cao J, Duan Y, Hui Y, Chuong TT, Ou D, Han F, Cheng F, Huang X, Wu B, Zheng N. High-efficiency, hysteresis-less, UV-stable perovskite solar cells with cascade ZnO–ZnS electron transport layer. *J Am Chem Soc.* 2018;141:541-547.
73. Kakavelakis G, Maksudov T, Konios D, Paradisanos I, Kioseoglou G, Stratakis E, Kymakis E. Efficient and highly air stable planar inverted perovskite solar cells with reduced graphene oxide doped PCBM electron transporting layer. *Adv Energy Mater.* 2017;7:1602120.
74. Cao J, Yin J, Yuan S, Zhao Y, Li J, Zheng N. Thiols as interfacial modifiers to enhance the performance and stability of perovskite solar cells. *Nanoscale.* 2015;7:9443-9447.

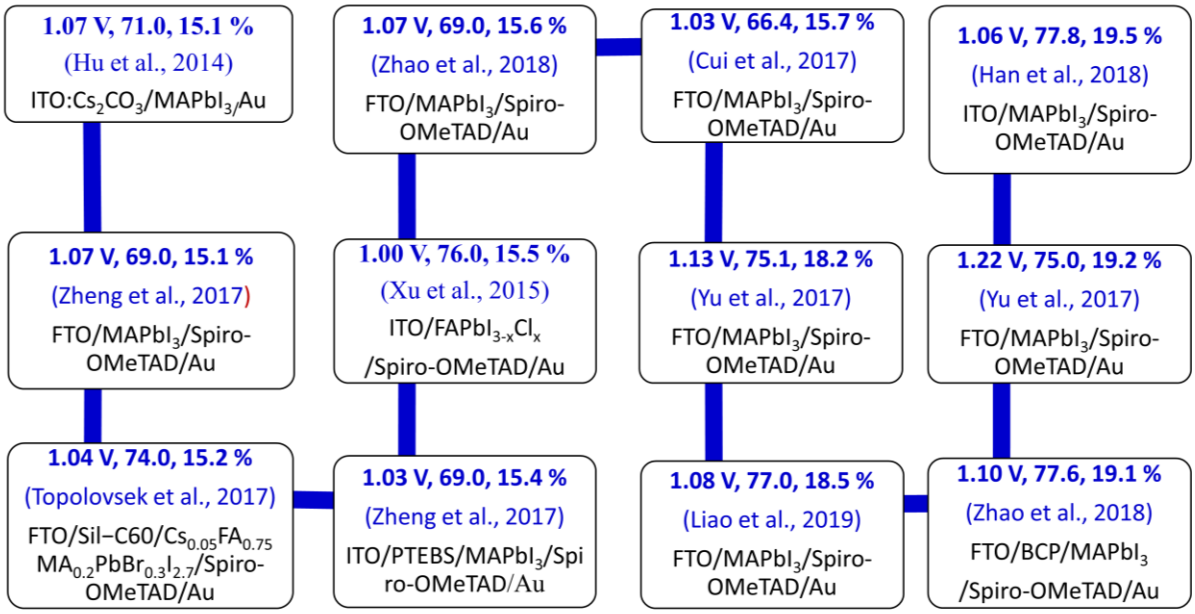

Fig. 1. Brief summary of ETL−free OIHP solar devices with PCE > 15%. V_{OC}, FF, PCE, author, year of publication, and architecture of each device are also provided [33,49−56].

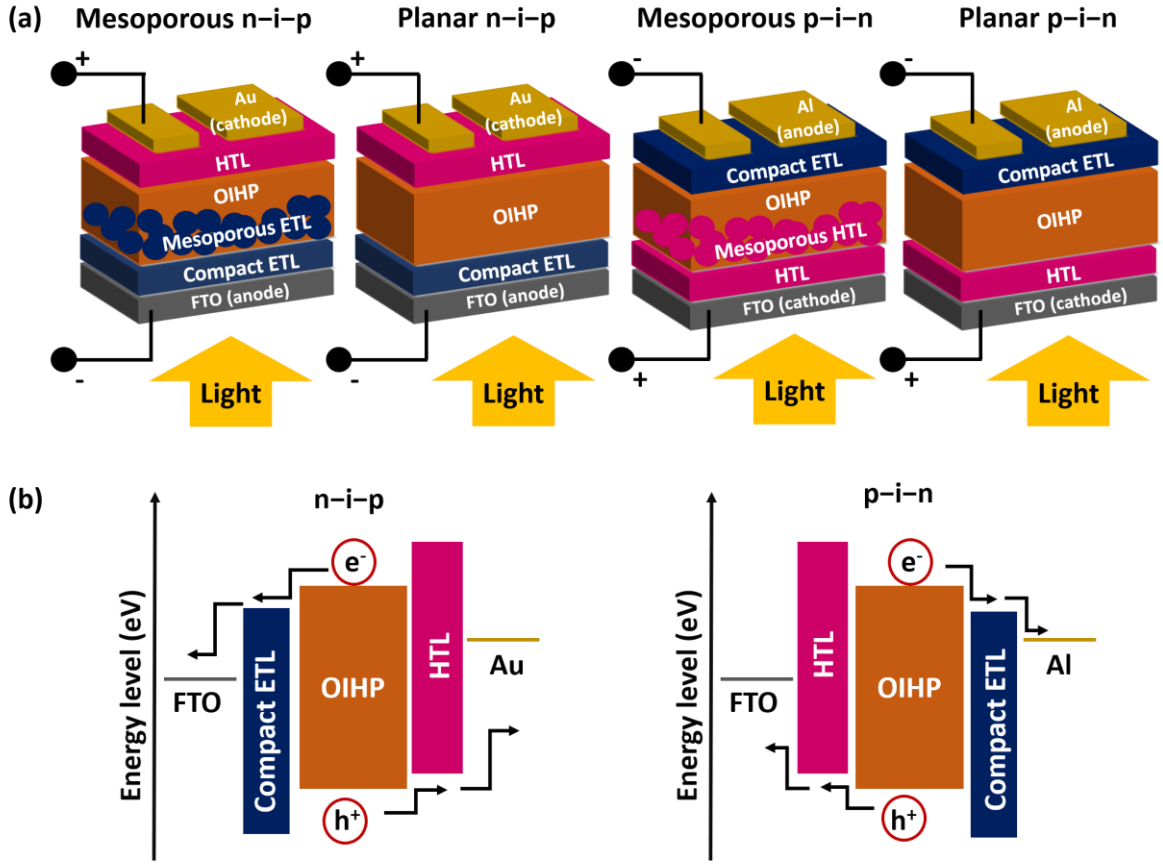

Fig. 2. (a) Device architectures of the mesoporous n–i–p, planar n–i–p, mesoporous p–i–n, and planar p–i–n OIHP structures. (b) Typical energy level alignments of the n–i–p and p–i–n device configurations.

Table 1. List of various TiO_2 based, SnO_2 based, and novel ETL OIHP solar cells. V_{oc}, FF, PCE, and architecture of devices are also provided [57−70].

ETL Type	ETL Composition	Device Architecture	V_{OC} (V)	FF	PCE (%)	Ref
TiO_2 based ETL	Rubidium chloride doped TiO_2 (RbCl-TiO_2)	FTO/RbCl−TiO_2/$MAPbI_{3-x}Br_x$/Spiro−OMeTAD/Ag	1.11	80.76	20.75	[57]
	Niobium doped TiO_2 (Nb−TiO_2)	FTO/Nb−TiO_2/$FA_{0.79}MA_{0.16}Cs_{0.05}Pb(Br_XI_{1-X})_3$/Spiro-OMeTAD/Au	1.09	78.0	21.3	[58]
	Chlorine doped TiO_2 (Cl−TiO_2)	ITO/Cl−TiO_2/$FA_{0.81}MA_{0.15}PbI_{2.55}Br_{0.45}$/Spiro−OMeTAD/Au	1.89	80.6	21.4	[59]
	Fluorine doped SnO_2 (F−SnO_2)	FTO/F−TiO_2/$(FAPbI_3)_{0.85}(MAPbBr_3)_{0.15}$/Spiro−OMeTAD/Au	1.13	78.1	20.2	[60]
SnO_2 based ETL	Graphene quantum dots doped SnO_2 (GQD−SnO_2)	ITO/GQD-SnO_2/$MAPbI_3$/Spiro−OMeTAD/Au	1.13	77.8	20.3	[61]
	SnO_2	ITO/SnO_2/$Cs_{0.05}(FA_{0.83}MA_{0.17})_{0.95}PbI_{2.55}Br_{0.5}$/Spiro−OMeTAD/Au	1.12	83.0	20.3	[62]
	SnO_2/Yttrium doped SnO_2 (Y−SnO_2)	FTO/SnO_2/Y−SnO_2/$Cs_{0.05}(FA_{0.83}MA_{0.17})_{0.95}PbI_{2.55}Br_{0.5}$/Spiro−OMeTAD/Au	1.12	78.2	20.6	[63]
	Chlorine−containing imidazole ionic liquid 4−imidazoleacetic acid hydrochloride doped SnO_2 (ImAcHCl−SnO_2)	FTO/ImAcHCl−SnO_2/$(FAPbI_3)_{0.95}(MAPbBr_3)_{0.05}$/Spiro−OMeTAD/Au	1.15	79.0	21.0	[64]
	Ethylene diamine tetraacetic acid doped SnO_2 (EDTA−SnO_2)	ITO/EDTA−SnO_2/$FA_{0.95}Cs_{0.05}PbI_3$/PCBM/Al	1.11	79.2	21.6	[65]
Novel ETL	c−TiO_2/WO_3	FTO/c−TiO_2/WO_3/$MAPbI_3$/Spiro−OMeTAD/Au	1.09	78.6	20.1	[66]
	SnS	ITO/SnS/$FA_{0.75}MA_{0.15}Cs_{0.1}PbI_{2.65}Br_{0.35}$/Spiro−OMeTAD/Au	1.16	73.0	20.1	[67]
	Nb_2O_5	FTO/Nb_2O_5/$CsFAMAPbI_{3-x}Br_x$/Spiro−OMeTAD/Au	1.19	78.6	20.2	[68]
	Choline chloride/C_{60}/BCP	ITO/PTAA/$CsFAMAPbI_{3-x}Br_x$/Choline chloride/C_{60}/BCP/Cu	1.14	78.0	21.0	[69]
	c−TiO_2/Lanthanum doped $BaSnO_3$ (La−$BaSnO_3$)	FTO/c−TiO_2/La−$BaSnO_3$/$MAPbI_3$/PTAA/Au	1.12	81.3	21.3	[70]

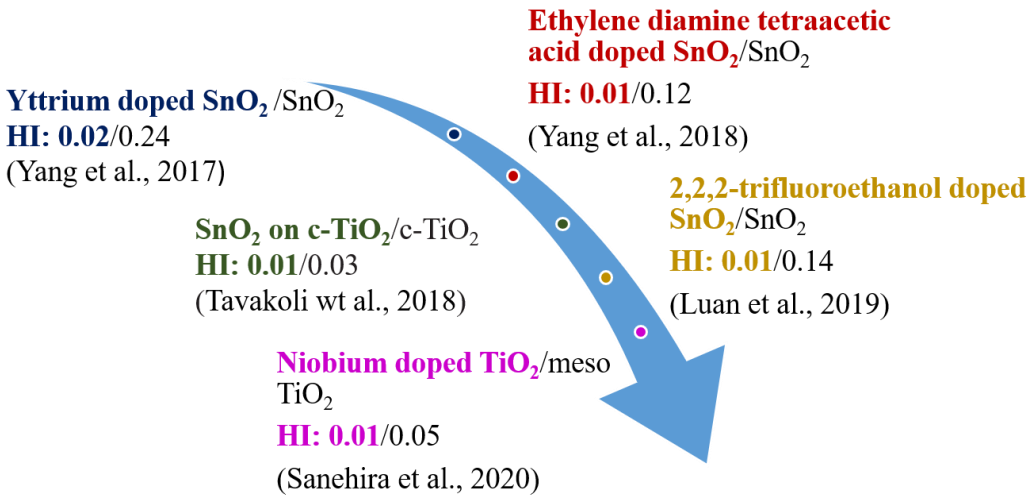

Fig. 3. Instances of reduced J−V hysteresis found in various doped ETL perovskite solar cells [26,38,39,58,71]. Hysteresis index (HI) is calculated using the formula: $HI = \frac{PCE_{reverse} - PCE_{forward}}{PCE_{reverse}}$ [59].

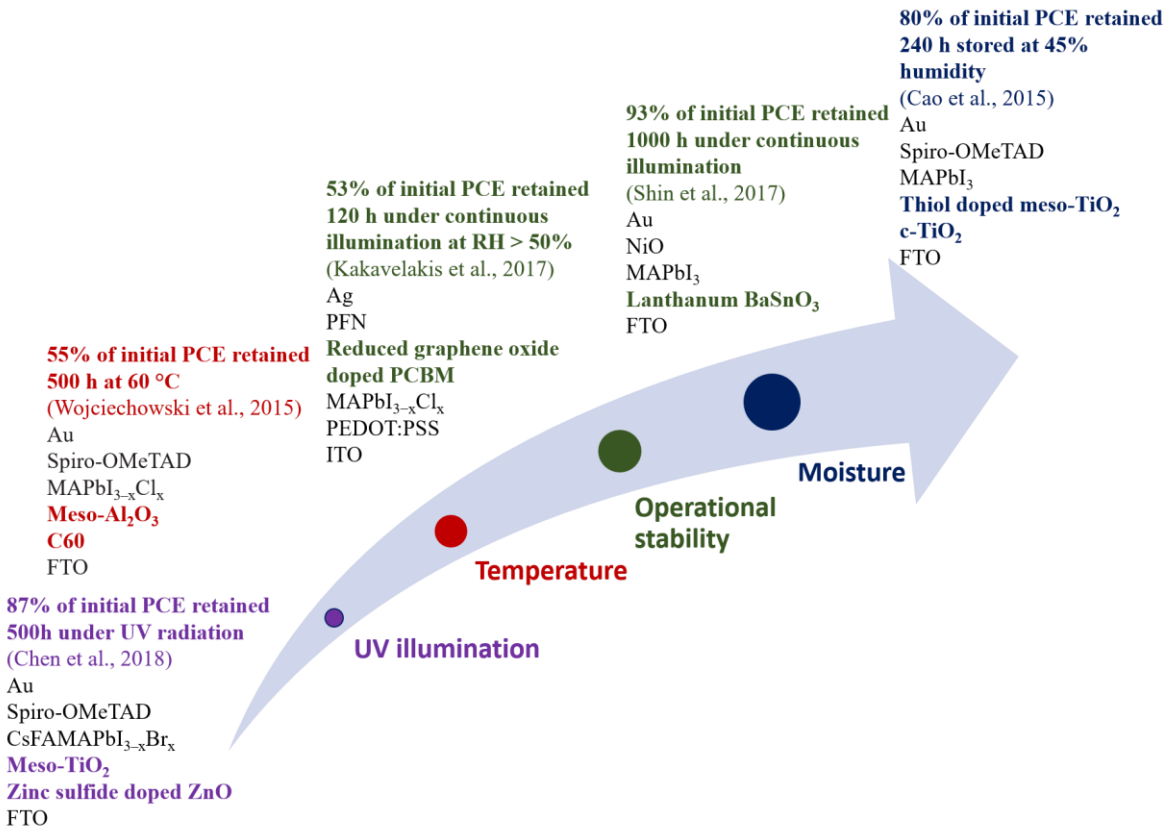

Fig. 4. Examples of perovskite solar devices containing various ETLs under different device stresses [37,70,72−74].